

# LIDAR INNOVATIONS FOR TECHNOLOGIES AND ENVIRONMENTAL SCIENCES (LITES) – AN REMOTE SENSING INFRASTRUCTURE FACILITY: SETUP AND MEASUREMENTS EXAMPLES

Boyan Tatarov<sup>1\*</sup>, Detlef Müller<sup>1</sup>, Matthias Tesche<sup>1,2</sup>, Sung-Kyun Shin<sup>1</sup>

<sup>1</sup>*School of Physics, Astronomy and Mathematics, University of Hertfordshire, College Lane, Hatfield, United Kingdom*

<sup>2</sup>*now at: Leipzig Institute for Meteorology (LIM), Leipzig University, Leipzig, Germany*

\*Email: [b.tatarov@herts.ac.uk](mailto:b.tatarov@herts.ac.uk)

## ABSTRACT

At the University of Hertfordshire, we have been developing a new remote sensing facility (LITES) to explore the feasibility of using Raman and/or fluorescence backscattering for chemical aerosol profiling. This paper provides an overview of the instruments of the facility and measurement examples. LITES includes a ultra-high-energy Nd:YAG/OPO setup, spectroscopic equipment with high spectral resolution, several imaging and single detectors that allow for time-resolved (lidar) signal detection, a Raman/fluorescence microscope, and a suite of gas and aerosol chambers. We present examples of elastic, rotational and vibrational spectroscopic lidar signals, as well as in-situ microscopic spectrums of dust and bio-aerosol compounds.

## 1. INTRODUCTION

Lidar is the only remote measurement method that allows for spatially (vertically) and temporally highly-resolved observations of atmospheric state parameters, trace gases and particulate pollution [1,2]. The combination of various lidar techniques (nitrogen Raman and high spectral resolution lidar) with mathematical inversion algorithms nowadays allows for temporally and vertically resolved observations of aerosol optical and microphysical properties [3,4,5]. Differential absorption lidar is another concept that allows for quantitative range-resolved measurements of the concentration of chemical components in the atmosphere [6]. However, lidar and passive remote sensing instruments currently cannot provide us with vertically-resolved information on the chemical composition of aerosols under ambient atmospheric conditions. We are exploring the potential of a multi-channel high-resolution spectrometric lidar for the vertically-resolved chemical characterization of aerosols and reactive gases by measuring range-resolved Raman and

fluorescence/photoluminescence spectra. For that purpose, we have been developing a new remote sensing facility, called Lidar Innovations for Technologies and Environmental Sciences (LITES). The facility combines a unique Lidar Spectroscopy Instrument (LiSsI) with in-situ instruments such as Raman and fluorescence microscope, gas and aerosol chambers.

In this work we present the setup of LITES and show measurement examples. LiSsI allows for the profiling of trace gases, chemical components in particles, and bio-aerosols in atmospheric aerosol pollution in the troposphere through combining different non-linear spectroscopy techniques (photoluminescence, fluorescence, Raman and coherent anti-Stokes Raman spectroscopy) on a single measurement platform.

## 2. INSTRUMENTS

The instruments of LITES were designed to operate as a single platform that allows for an easy switch between different experimental setups. Most of the equipment parts can be used for more than one instrument component of LITES. Table 1 summarizes the specifications of the system.

### 2.1 The lidar system

The main components of the lidar subsystems include:

- an ultra-high-energy seeded Nd:YAG laser (Continuum Powerlite Furie LD) with SHG and THG. This system emits laser light with energies up to 8 J per pulse (at the fundamental 1064-nm wavelength). This output corresponds to a pulse power of more 500 GW and an average power of more than 50 W;
- an Optical Parametric Oscillator (Horizon OPO) that is optically pumped by the main laser. The OPO emits laser light from the deep UV (192 nm) to the near infrared (2750 nm);

**Table 1.** Technical specification of the lidar systems

Continuum Powerlite Furie LD	
Laser type	Nd:YAG, injection seeded
Pulse energy	8000 mJ@1064 nm 5000 mJ@532 nm 2500 mJ@355 nm
Beam divergence	0.5 mrad
Repetition rate	10 Hz
Linewidth	<0.003 cm <sup>-1</sup>
Pulse duration	<15 ns
Horizon Optical Parametric Oscillator	
Pump wavelength	355 nm
Wavelengths	from 192 to 2750 nm
Resolution/Scan step	0.01 nm
Pulse energy	120 mJ@400 nm 60 mJ@600 nm 25mJ@300 nm
Beam divergence	<2 mrad (both axes)
Repetition rate	10 Hz
HORIBA 1250M Research Spectrometer	
Focal length	1.25 m, F/9
Spectral range	0-1500 nm @ 1200 g/mm
Grating size	110 mm x 110 mm
Dispersion @500 nm	0.65 nm/mm
Accuracy/Repeatability	±0.15 nm / ±0.005 nm
Gratings and blaze	max resolutions at 313.183 nm
2400 gr/mm @250 nm	0.003 nm
1800 gr/mm @ 400 nm	0.004 nm
1200 gr/mm @ 330 nm	0.006 nm
600 gr/mm @ 500 nm	0.012 nm
Detection	
Mie and Rayleigh scattering	355 nm, PMT HV-R9880U-20 532 nm, PMT HV-R9880U-20 1064 nm, APD InGaAs50, Si
Spectroscopic 1 Licel SP32-20	Hamamatsu H7260-20, 0.8 mm x 7 mm x 32 anodes spectral response 300-920 nm
Spectroscopic. 2 Princeton Instruments PI-MAX4 ICCD camera	Number of pixels 1024x1024 Pixels size 16 x 16 μm Gen III filmless intensifier Sensitive range 290-710 nm
Spectroscopic 3 ANDOR iXon 3 EMCCD camera	Number of pixels 512x512 Pixels size 12.8 x 12.8 μm Sensitive range 300-710 nm
Schmidt-Cassegrain Telescope	
Primary	f/10, FL=3910 mm, D=391mm
Second	f/10, FL=2000 mm, D=200mm
Data acquisition system	
Mie and Rayleigh scattering	Licel transient recorders, 16-bit, 20 MHz A/D converters and photon-
Multi-anode PMT	Single-photon counting, maximum count rate 100 MHz, 50 ns
ICCD	Digitization 16 bit, 32 MHz, minimum gate width 2 ns
EMCCD	Digitization 16 bit, 17 MHz

- a customized motorized beam combiner for selecting the wavelengths. The beam combiner allows for switching between seven modes, namely emission of 1) 1064 nm only, 2) 532 nm only, 3) 355nm only, 4) 1064 nm and 532 nm (simultaneously), 5) 1064 nm and 532 nm and 355 nm (simultaneously), as well as 6) optimized OPO pumping, and 7) side-port emission of laser light for non-lidar applications;

- a Horiba 1250M imaging spectrometer with four exchangeable gratings, dual entrance ports/slits and two exits ports – one imaging (front) and one high-spectral resolution (side) port/slit;

- three imaging detectors that can be used with the spectrometer;

- an intensified CCD camera (ICCD, Princeton Instruments PI-MAX4 1024i-HBf);

- a 32-channel Licel PMT;

- an EMCCD (ANDOR iXon 3);

- three kinds of single detectors – Photomultiplier tubes, InGaAs ADP, and silicon diode.

The system allows for using three types of acquisition approaches by which we can detect lidar signal on the basis of a) the use of single detectors, b) simultaneous detection of multi-channel spectroscopically-resolved lidar signals, c) determination of Raman/fluorescence spectrums by point-to point swapping of wavelengths, d) swapping of the range of wavelengths for the imaging detectors we use for LITES.

Depending on the setup of the experiment, the lidar instrument can be used as a a) multiwavelength elastic backscatter lidar for measurements of aerosols and temperature from the troposphere to the mesosphere, b) multi-channel spectroscopic Raman lidar (using Stokes and anti-Stokes, rotational, and rotational-vibrational Raman scattering), c) multi-channel spectroscopic photoluminescence/fluorescence lidar, d) high spectral resolution lidar (HSRL), e) polarization lidar, or f) infrared absorption and differential absorption lidar (DIAL).

## 2.2 The Raman and fluorescence microscope

This instrument allows for investigations of Raman and fluorescence spectrums of solid-state aerosol samples taken by in-situ particle-collection methods. The instrument is based on an

Olympus BX51TRF-6 microscope. The microscope can use the OPO laser emissions or light from a 532-nm CW DPSS laser that is used as pumping source for delivering Raman and fluorescence spectrums. The microscope is equipped with objective lenses with magnification factors x5, x10, x20, x50, and x100. In that way we obtain a spatial resolution better than  $1\mu\text{m}$ . An additional CMOS imaging camera (xiQ, MQ013CG-) is available for acquiring high spatial resolution reflection or transmission images of the samples in the visible range of radiation. The spectrums can be obtained with the main spectrometer HORIBA 1250M and all detection systems available in the LITES facility.

### 2.3 Customized gas and aerosols gas chambers

LITES also includes a suite of gas and aerosol chambers for the investigation of general optical properties of gases and particles, namely ATR (Attenuation, Transmission, Reactance) and Raman and fluorescence spectrums of gases and aerosols particles. The chambers can simulate the conditions of gas mixtures of different types of air-pollutions, reactive trace gases and aerosol particles under real atmospheric conditions up to tropopause heights.

## 3. RESULTS

### 3.1 Elastic analog and photon counting signals

Figure 1 shows an example of lidar signals measured by the elastic configuration of LITES on 7 March 2018. The red curves present signals taken from 1930 - 2130 UTC with 100 mJ laser emission power. The black curves present the analog and photon counting signals obtained from 2312 - 2334 UTC on the same date with 500 mJ laser emission power

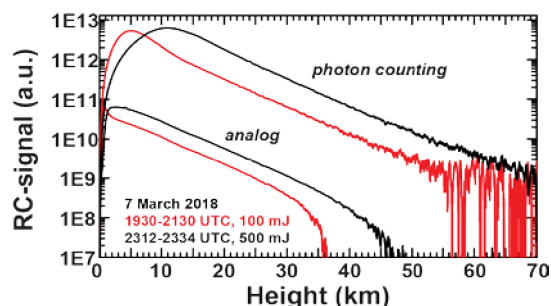


Figure 1. Example of a LITES measurement (elastic signals) at 532 nm taken on 7 March 2018.

### 3.2 Pure rotational and vibrational-rotational signals

Results of the first pure-rotational Raman scattering measurements that were obtained with the ICCD camera and the Horiba 1250M spectrometer are presented in Figure 2. The emitted laser intensity was 300 mJ at 354.9 nm. The spectrum was averaged over 10 laser shots and the background has been subtracted. The time gate of the camera was set to 0.03-2.00  $\mu\text{s}$  which corresponds to 4.5-300.0 m distance (black curve) and 2-4  $\mu\text{s}$  which corresponds to 300-600 m distance (red curve). A 355-nm RazorEdge ultrastep long-pass edge filter (Semrock LP02-355RE-25) was used to suppress elastic scattering. The spectrometer grating was set to 1200 g/mm with a 50  $\mu\text{m}$  entrance slit that allows for a spectral resolution of less than  $5\text{ cm}^{-1}$ .

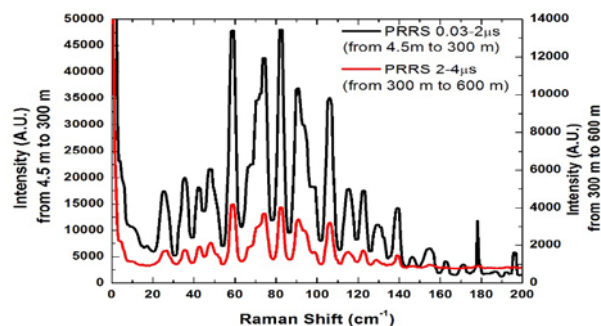


Fig. 2. Pure rotational Raman spectrum of air at 2017 UTC on 4 November 2017 averaged over 10 shots (1 s).

An example of spectra taken with the rotational-vibrational lidar Raman set-up is shown in Fig. 3.

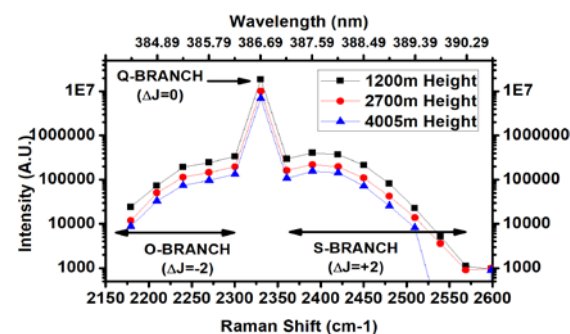


Fig. 3. Rotational-vibrational Raman spectrum of air nitrogen molecules taken from 2030 to 2359 UTC on 19 October 2018 averaged over 125576 shots (209 minutes). Laser power: 1100 mJ at 354.9 nm. Grating: 1200 g/mm. Entrance slit: 50  $\mu\text{m}$ . Resolution  $\approx 5\text{ cm}^{-1}$ .

### 3.3 Nitrogen dioxide measurements

Figure 4 shows one of the first LiSsI Raman measurements performed between 1726 and 1735 UTC on 3 November 2017 using the laser at 354.9 nm with a power of approximately 300 mJ. The signals were taken with a SP32-20 multi-channel PMT in photon counting mode and averaged over 5400 laser shots.

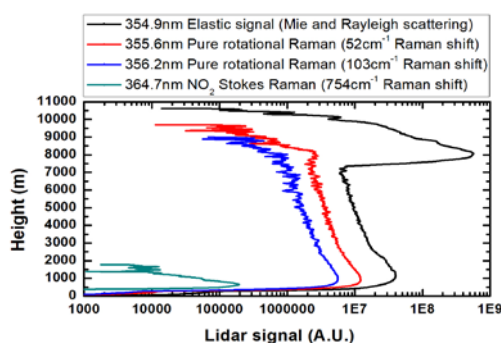


Figure 4. Elastic and Raman lidar signals at 1726 UTC on 3 November 2017.

The spectrometer grating was set to 1200 g/mm with a 50- $\mu$ m entrance slit. Aerosols can be seen in the elastic signal (354.9nm) up to 3-km height above ground. Cirrus clouds are clearly visible between 7.0 and 10.5 km height. Profiles from pure rotational Raman lidar signals from nitrogen molecules were detected at two wavelengths up to approximately 9 km height. Raman signals were also observed in the 364.7-nm channel (754  $\text{cm}^{-1}$  Raman shift) up to 1.4 km height. This signal is most probably caused by nitrogen dioxide ( $\text{NO}_2$ ) which has a strong Raman peak at 754  $\text{cm}^{-1}$ .

### 3.4 Microscopic Raman spectra of standard samples and mineral dust

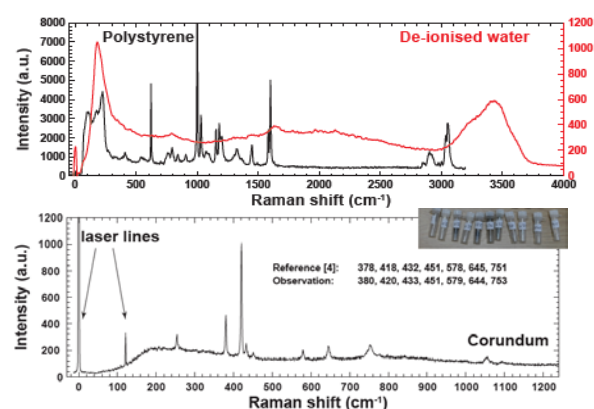


Figure 5. Raman spectrums of: a) polystyrene and de-ionized water and b) corundum ( $\text{Al}_2\text{O}_3$ )

Figure 5 presents examples of Raman spectrums obtained by the Raman microscope of calibration standard samples (polystyrene and de-ionized water) and corundum ( $\text{Al}_2\text{O}_3$ ). The spectral resolution is 0.02nm, we used 150mW@532nm laser power and a grating with 2400gr/mm and slit width of 200 $\mu$ m.

### 3.5 Microscopic fluorescence spectra of bioaerosols.

Figure 6 presents examples of measurements of fluorescence spectra of different types of fresh (Cupressus) and aged (Platanus, Cupressus,) pollen taken from different urban locations at the city of Granada (Spain, 680 m a.s.l.). The spectra were obtained using the laser wavelength 532 nm, a grating with 2400 grooves  $\text{mm}^{-1}$ , and 200  $\mu$ m slit width. Gold-coated slides (up to 50-nm thick coating) were used to improve signal intensity.

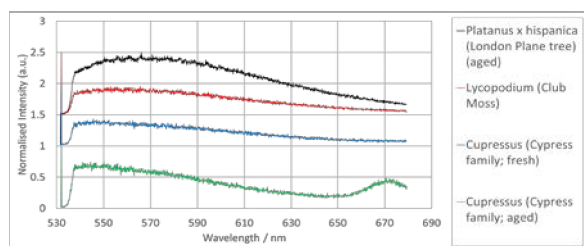


Figure 6. Fluorescence spectra of fresh and aged pollen.

### ACKNOWLEDGEMENTS

This work was supported by the University of Hertfordshire through capital investment and the proof-of-concept grant MARBLE. Boyan Tatarov is supported by a Marie-Sklódowska-Curie Action Fellowship of the European Commission (CAPABLE, H2020-MSCA-IF-2015).

### REFERENCES

[1] C. Weitkamp: Springer, New York 2005, ISBN 0-387-40075-3.  
 [2] R. M. Measures, Laser Remote Sensing, 510 pp., John Wiley, New York, 1984  
 [3] A. Ansmann, M. Riebesell, and C. Weitkamp, Optics Letters, 15 (1990) 746.  
 [4] P. Piironen and E. W. Eloranta, Optics Letters, 19 (1994) 234.  
 [5] D. Müller, et al., Applied Optics, 38 (1999) 2346.  
 [6] Bösenberg, J., Springer Series in Optical Sciences, Springer-Verlag, New York, 2005.